THE JOURNAL OF PHYSICAL CHEMISTRY A
A JOURNAL OF THE AMERICAN CHEMICAL SOCIETY

pubs.acs.org/JPCA Article

A Charge−Charge Flux−Dipole Flux Analysis of Simple Molecular Systems with Halogen Bonds

Paulo Eduardo Cavalcanti Martins Filho and Roberto Luiz Andrade Haiduke*

Cite This: https://doi.org/10.1021/acs.jpca.3c08229 Read Online

ACCESS | Metrics & More | Article Recommendations | Supporting Information

ABSTRACT: The presence of halogen bonds (R−X···B; R = substituent group, X = halogen, and B = Lewis base) provides quite amazing molecular systems for electronic structure investigations, presenting unique characteristics of fundamental relevance to supramolecular chemistry among other areas. Here, we use a double-hybrid approach from Density Functional Theory and triple-ζ basis sets augmented with diffuse functions (B2PLYP/def2-TZVPD) to deal with a large group of simple molecular systems containing halogen bonds (XBs), focusing on geometrical structures, binding energies, harmonic vibrational frequencies, and fundamental infrared intensities. Next, the electron densities and their variations on vibrations are carefully studied with the Quantum Theory of Atoms in Molecules (QTAIM) formalism and the charge−charge flux−dipole flux (CCFDF) model. We notice that the R−X stretching mode usually shows vibrational frequency decrements and infrared intensifications during the XB formation. Such features were also observed in hydrogen bonds, although the explanation for the band strengthening is different. Surprisingly, the most important contribution to these intensity increments due to complexation is now the interaction term between the charge flux and dipole flux (CF × DF). Thus, the use of atomic dipoles is mandatory to fully understand this phenomenon. In fact, the huge charge flux contributions to changes in dipole moment derivatives of R−X stretchings on halogen bonding are no longer accompanied by opposite variations of similar magnitudes in polarizations described by atomic dipole fluxes, which provided nearly unaltered values during the XB formation. Thus, the electronic charge flux direction change that takes place in complexes (from B to R) now reinforces dipole moment derivative terms from such atomic polarizations (mainly from the X atom). This intermolecular charge flux seems to be responsible for the unusual features noticed in the R−X stretching mode with the CCDDF/QTAIM model.

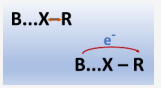

INTRODUCTION

Halogen bonds (XBs) are attractive interactions (intra- or intermolecular) between a halogen atom (X) bonded within a system (R−X), acting as a Lewis acid, and a Lewis base moiety (B), being schematically represented by R−X···B. The R−X unit is also known as the XB donor, while B is the XB acceptor.[1−3] The origin of this interaction is closely linked to the σ-hole concept,[4] which is evidenced in the halogen atom due to the formation of a chemical bond with R, although there are some XB complexes presenting features that cannot be simply explained by the σ-hole model.[5] This leads to important electrostatic contributions to XBs, although charge transfer and dispersion/polarization effects are also mentioned as relevant factors to understand this kind of interaction.[1] Thus, the asymmetry of the electron cloud of the halogen atom involved in a chemical bond is fundamental here.[1−3] In fact, large covalent contributions are evidenced in the strongest XBs, which are explained by means of a three-center-four-electron (3c-4e) mechanism due to electronic charge donation from the lone pair of the Lewis base to the unoccupied antibonding σ orbital (σ*) of the R−X moiety,[3,6,7] being majorly associated with the charge transfer values observed.[3] As a result, the strength of XBs can range from 10 to 200 kJ mol^{-1}.[2] The investigations indicated that the forces of XBs or the σ-hole magnitudes tend to increase with the halogen polarizability (F < Cl < Br < I) and when this X atom is bonded to a more electron withdrawing moiety (R).[1,2,8] Indeed, halogens bonded to some groups with very small electron withdrawing capabilities do not present a σ-hole, exhibiting instead an electrostatic potential minimum.[8]

Nowadays, the XB interactions are gaining more and more attention mainly because of their role in the supramolecular chemistry area.[1,2] However, halogen bonding is obviously important in biomolecular chemistry, providing a potential path for drug design, and there are many studies for applications of these interactions in catalysis and material sciences as well.[1] Interestingly, XBs are also effective in binding anions of solutions or solids, which is linked to the fact that anions commonly provide better XB acceptors than neutral systems.[2] There are a few contrasts between halogen bonding and traditional hydrogen bonds (HBs). For example, XBs can be stronger and exhibit larger covalent character than HBs in comparable complexes.[6,7] However, many features of both these interactions present remarkable similarities, such as in spectroscopic trends, for example.[2,9]

Received: December 22, 2023
Revised: February 26, 2024
Accepted: February 27, 2024

There are some fundamental studies regarding XBs in the literature that can be mentioned in this work. For example, Anderson et al. analyzed the quite important XB18 and XB51 benchmark sets[10] and provided corrections to inconsistencies seen in binding energy values of XB51.[11] Another investigation was focused on the distinct dimers that may be obtained from the combination between HCN and HX (X = F, Cl, Br, and I).[12] Along with the traditional HB interactions, which provided the global minima in all of these systems, the authors also identified competitive minimum structures ascribed to XB complexes and calculated binding energies with accurate treatments.

Certainly, as mentioned above, the electron density properties of halogen bonding complexes deserve detailed investigations. Therefore, the Quantum Theory of Atoms in Molecules (QTAIM)[13,14] is able of providing a powerful tool for the analysis of electronic structures, furnishing an atomic partition of electric properties, for example. In addition, QTAIM quantities obtained at bond critical points (BCPs) can be quite helpful to these studies, as well, especially in dimers. Thus, atomic charges (q) and atomic dipole components (m_x, m_y, and m_z) are available and can be used to achieve the Cartesian components of the molecular dipole moment (μ_x, μ_y, and μ_z). For example,

$$\mu_z = \sum_i q_i z_i + \sum_i m_{i,z} \quad (1)$$

where the sums are performed for all the i atoms of the molecular system. See that the charges must be multiplied by the position along the axis (z_i) to provide dipole moment contributions. Atomic charges weighted by nuclear positions constitute an obvious contribution to dipole moments that refers to electronic charge transfers between atoms as molecular systems are formed. However, atomic dipoles may be quite important to electric properties once these quantities describe atomic polarizations along the formation of chemical bonds. This formally exact electrical decomposition is based on the concept of zero-flux surfaces from QTAIM.[13,14] Of course, similar expressions hold for the other components of the molecular dipole moment.

The derivatives of eq 1 during the displacement of an atom (a) along the z or x axis provide polar tensor components (p) given by

$$p_{zz}^{(a)} = \frac{\partial \mu_z}{\partial z_a} = q_a + \sum_i \frac{\partial q_i}{\partial z_a} z_i + \sum_i \frac{\partial m_{i,z}}{\partial z_a} \text{and} \quad (2)$$

$$p_{zx}^{(a)} = \frac{\partial \mu_z}{\partial x_a} = \sum_i \frac{\partial q_i}{\partial x_a} z_i + \sum_i \frac{\partial m_{i,z}}{\partial x_a} \quad (3)$$

with analogous expressions for the remaining atomic polar tensor (APT) elements.[15] The terms at the right of eq 2 are labeled as charge (C), charge flux (CF), and atomic dipole flux (DF) contributions to $p_{zz}^{(a)}$, respectively, while only charge flux and dipole flux are observed for $p_{zx}^{(a)}$. This provides a quite reliable model for dipole moment derivatives.

Certainly, there are equivalent expressions for the dipole moment derivatives in terms of each i normal mode (Q_i) achieved by customary matrix transformations from the vibrational analysis on the molecular polar tensor (juxtaposition of APTs),[16]

$$\frac{\partial \mu_z}{\partial Q_i} = \sum_j q_j \frac{\partial z_j}{\partial Q_i} + \sum_j \frac{\partial q_j}{\partial Q_i} z_j + \sum_j \frac{\partial m_{j,z}}{\partial Q_i} = \left(\frac{\partial \mu_z}{\partial Q_i}\right)_C + \left(\frac{\partial \mu_z}{\partial Q_i}\right)_{CF} + \left(\frac{\partial \mu_z}{\partial Q_i}\right)_{DF} \quad (4)$$

Notice that the charge term is now weighted by atomic displacements in that particular normal mode.

Thus, the infrared intensity (A_i) for Q_i can be obtained with the help of quantities achieved by means of eqs 2−4, as provided by the charge−charge flux−dipole flux (CCFDF) model.[15] Therefore, the infrared intensities are readily evaluated in terms of charge (C), charge flux (CF), dipole flux (DF), and cross products between pairs of these contributions (C × CF, C × DF, and CF × DF),

$$A_i = \frac{N_A \pi}{3c^2}\left[\left|\left(\frac{\partial \vec{\mu}}{\partial Q_i}\right)_C\right|^2 + \left|\left(\frac{\partial \vec{\mu}}{\partial Q_i}\right)_{CF}\right|^2 + \left|\left(\frac{\partial \vec{\mu}}{\partial Q_i}\right)_{DF}\right|^2 + 2\left(\frac{\partial \vec{\mu}}{\partial Q_i}\right)_C \cdot \left(\frac{\partial \vec{\mu}}{\partial Q_i}\right)_{CF} + 2\left(\frac{\partial \vec{\mu}}{\partial Q_i}\right)_C \cdot \left(\frac{\partial \vec{\mu}}{\partial Q_i}\right)_{DF} + 2\left(\frac{\partial \vec{\mu}}{\partial Q_i}\right)_{CF} \cdot \left(\frac{\partial \vec{\mu}}{\partial Q_i}\right)_{DF}\right] \quad (5)$$

where c and N_A refer, respectively, to the light speed and Avogadro number.[17] Hence, more succinctly,

$$A_i = A_i^C + A_i^{CF} + A_i^{DF} + A_i^{C\times CF} + A_{C\times DF}^i + A_i^{CF\times DF} \quad (6)$$

The CCFDF/QTAIM model has being applied to several systems, including dimers with hydrogen bonds (X−H··· Y).[18−20] These studies were focused on understanding the origin of the large infrared strengthening normally observed in the X−H stretching mode due to dimerization, which indicates that the charge−charge flux term normally plays a major role. In other words, the presence of an HB induces a charge flux change in the dimer that is coordinated with the static charge movement in this vibrational mode. However, although there is some previous research discussing that infrared intensities of the R−X stretching are also enhanced on halogen bonding,[21−25] none of these works considered the role of atomic dipoles and their fluxes.

Hence, this study is focused on investigating the XBs in a large group of simple systems by means of Density Functional Theory (DFT) calculations and QTAIM quantities, with special attention to variations in fundamental infrared intensities of the R−X stretching mode on complexation by means of XB formation. The charge transfer between the monomers and descriptors obtained at the BCPs of XBs is also evaluated.

METHODS

Most of the electronic structure calculations were performed within the Gaussian 09 package.[26] The equilibrium geometries were obtained by means of Density Functional Theory (DFT) calculations done with the B2PLYP exchange-correlation functional[27] and def2-TZVPD basis sets,[28−30] as retrieved from the Basis Set Exchange database.[31] Tighter optimization

https://doi.org/10.1021/acs.jpca.3c08229
J. Phys. Chem. A XXXX, XXX, XXX−XXX

Table 1. Some Equilibrium Geometrical Data and Binding Energies (BEs) for the Complexes with Halogen Bonds Investigated Here (R−X···B) along with the Electron Density at the XB BCP (ρ_{BCP}) and the QTAIM Charge Transfer (CT) between Monomers as Obtained at the B2PLYP/def2-TZVPD Level[f]

	this work							previous investigations		
complex	$r_{X\cdots B}$ (Å)	r_{R-X} (Å)	θ_{RXB} (deg)	BE (kcal mol^{-1})	ρ_{BCP} (a.u.)	CT (e)[a]	BE [DLPNO-CCSD(T)/CBS] (kcal mol^{-1})	$r_{X\cdots B}$ (Å)	θ_{RXB} (deg)	BE (kcal mol^{-1})
HCl···Cl$^-$	3.335	1.284	180.0	1.13	0.0094	0.043	1.36			
HCl···Br$^-$	3.570	1.283	180.0	0.65	0.0075	0.040	1.04			
HCl···I$^-$	3.881	1.282	180.0	0.19	0.0056	0.038	0.58			
HBr···Cl$^-$	3.176	1.438	180.0	4.73	0.0155	0.072	4.52			
HBr···Br$^-$	3.393	1.436	180.0	3.73	0.0126	0.068	3.73			
HBr···I$^-$	3.686	1.433	180.0	2.73	0.0096	0.067	2.61			
HI···Cl$^-$	3.078	1.651	180.0	11.02	0.0234	0.112	11.95			
HI···Br$^-$	3.285	1.646	180.0	9.17	0.0194	0.111	10.42			
HI···I$^-$	3.556	1.642	180.0	7.30	0.0154	0.113	7.84			
FCl···Cl$^-$	2.304	1.899	180.0	34.05	0.0831	0.485	29.52	2.334,[b] 2.316[c]	180.0[c]	43.9,[b] 28.98[c]
FCl···Br$^-$	2.442	1.913	180.0	31.97	0.0727	0.542	27.99	2.473[b]		40.5[b]
FCl···I$^-$	2.595	1.953	180.0	31.28	0.0653	0.648	26.28	2.637[b]		38.7[b]
FBr···Cl$^-$	2.435	1.983	180.0	39.34	0.0707	0.412	36.18	2.454[b]		48.7[b]
FBr···Br$^-$	2.583	1.989	180.0	36.70	0.0618	0.461	34.15	2.601[b]		44.7[b]
FBr···I$^-$	2.755	2.012	180.0	35.05	0.0551	0.547	31.24	2.775[b]		42.4[b]
FI···Cl$^-$	2.596	2.092	180.0	43.36	0.0595	0.330	43.56	2.620[b]		49.8[b]
FI···Br$^-$	2.757	2.093	180.0	39.95	0.0518	0.372	41.02	2.781[b]		45.1[b]
FI···I$^-$	2.950	2.102	180.0	37.22	0.0457	0.441	36.97	2.977[b]		41.9[b]
Br_2···NCH	2.889	2.309	180.0	3.38	0.0159	0.017	3.12			3.63, 3.61[d]
Br_2···PCH	3.553	2.300	180.0	0.77	0.0074	0.012	1.14			1.18[d]
BrI···NCH	2.859	2.503	180.0	5.36	0.0211	0.020	5.27			5.31[d]
ClBr··· NCH	2.807	2.166	180.0	4.14	0.0187	0.022	3.81			4.47[d]
ClI···NCH	2.783	2.355	180.0	6.28	0.0242	0.024	6.23			6.31[d]
FBr··· NCH	2.515	1.795	180.0	7.34	0.0339	0.048	6.80			7.61, 7.53[d]
FI···NCH	2.573	1.950	180.0	9.49	0.0364	0.036	9.67			9.45, 9.33[d]
HBr··· NCH	3.322	1.421	180.0	0.99	0.0066	0.003	1.30	3.24[e]	180.0[e]	1.41,[d] 1.54[e]
HI···NCH	3.315	1.612	180.0	1.94	0.0087	0.002	2.27	3.26[e]	180.0[e]	2.24,[d] 2.74[e]
I_2···NCH	2.998	2.689	180.0	3.93	0.0162	0.013	4.26			4.03[d]
FCl··· NCH	2.550	1.657	180.0	5.01	0.0268	0.041	4.52			4.81[d]
FI···PCH	3.051	1.936	180.0	2.49	0.0239	0.038	2.89			2.74[d]
FBr···PCH	3.042	1.781	180.0	1.64	0.0195	0.045	1.62			2.07[d]
FCl···PCH	3.188	1.643	180.0	0.86	0.0118	0.028	1.04			1.16[d]
CH_3I···Cl$^-$	3.046	2.189	180.0	8.08	0.0251	0.126	9.02			
CH_3I···Br$^-$	3.253	2.184	180.0	6.38	0.0207	0.124	7.60			
CH_3I···I$^-$	3.520	2.181	180.0	4.73	0.0166	0.128	5.37			
CF_3Cl··· Cl$^-$	2.956	1.741	180.0	9.77	0.0204	0.090	10.03			
CF_3Cl··· Br$^-$	3.165	1.741	180.0	8.33	0.0164	0.085	8.87			
CF_3Cl···I$^-$	3.444	1.743	180.0	6.80	0.0126	0.081	6.97			
CF_3I···Cl$^-$	2.825	2.201	180.0	23.37	0.0386	0.203	23.91			
CF_3I···Br$^-$	3.011	2.200	180.0	20.49	0.0326	0.214	21.51			
CF_3I···I$^-$	3.244	2.203	180.0	17.61	0.0273	0.235	17.88			

[a]Electronic charge transfer from the XB acceptor (Lewis base) to the XB donor (Lewis acid). [b]Theoretical values from ZORA-BP86/TZ2P calculations mentioned in ref 7. [c]Theoretical values from CCSD(T)/aug-cc-pVTZ calculations mentioned in ref 6. [d]Theoretical values from CCSD(T)/CBS and CCSD(T)/AVTZ calculations mentioned in ref 11. [e]Theoretical values from CCSD(T)/ha5Z calculations mentioned in ref 12. [f]BE values from DLPNO-CCSD(T)/CBS calculations are also presented.

criteria (opt = tight) and denser integration grids (grid = ultrafine) were selected for these calculations. These equilibrium geometries are collected in Table S1 (see the Supporting Information). In the sequence, wave function files were generated with the appropriate density matrix for the B2PLYP/def2-TZVPD method (density = current)[32−35] at the equilibrium geometries found previously and also for distorted geometries with atomic displacements of ±0.01 Å, which requires $6N + 1$ (N = number of atoms) calculations without symmetry considerations (also using the same denser grid mentioned before). Next, these files were used inside AIMAll[36] for attaining atomic charges and atomic dipoles from QTAIM,

https://doi.org/10.1021/acs.jpca.3c08229
J. Phys. Chem. A XXXX, XXX, XXX−XXX

which are employed in numerical derivative calculations of these quantities with the customary two-point approach.

Some complete basis set (CBS) extrapolations of electronic energies obtained by means of the domain-based local pair natural orbital coupled cluster method with single, double, and perturbative triple excitations [DLPNO-CCSD(T)][37,38] were also done within Orca 5.0.4[39,40] by using the previous B2PLYP/def2-TZVPD equilibrium structures. Hence, def2-TZVPP and def2-QZVPP basis sets are used[28] in these calculations along with def2/J, def2/JK, def2-TZVPP/C, and def2-QZVPP/C auxiliary sets.[41−43] Self-consistent-field and correlation energy extrapolations are done according to default options, using extrapolation schemes[44,45] and exponents[46] implemented inside Orca 5.0.4.

RESULTS AND DISCUSSION

Geometries and Binding Energies. As seen in Table 1, the XBs investigated in this study are characterized as linear intermolecular interactions with X···B bond lengths ($r_{X\cdots B}$) between 2.3 and 3.9 Å, respectively, for FCl···Cl$^-$ and HCl···I$^-$ complexes. The R−X bond lengths (r_{R-X}) are also displayed in Table 1 for reference. First, one can notice that our B2PLYP/def2-TZVPD calculations exhibit a nice agreement with high-quality theoretical values available for binding energies (BEs) and X···B distances,[6,11,12] as seen in Table 1. However, the ZORA-BP86/TZ2P values found for BEs[7] are systematically larger than ours. The BEs from the B2PLYP/def2-TZVPD results are also in nice accordance with the DLPNO-CCSD(T)/CBS values obtained here, with a mean absolute deviation (MAD) of 0.93 kcal mol^{-1}. These comparisons indicate that our computational protocol is adequate for evaluating halogen bonding with a reasonable demand for computational resources that allows achieving the posterior vibrational calculations and CCFDF/QTAIM partitions. The BEs obtained vary from very weak (0.19 kcal mol^{-1} for HCl··· I$^-$) to quite strong (43.36 kcal mol^{-1} for FI···Cl$^-$) intermolecular interactions. Hence, the interactions with anions as Lewis bases can provide almost insignificant BEs to the strongest XBs investigated depending on the donor monomer and base efficiency for electronic charge donation. In fact, the highest BE values obtained here are those of F−X′···X$^-$ and F_3C−I···X$^-$ complexes (X, X′ = Cl, Br, or I).

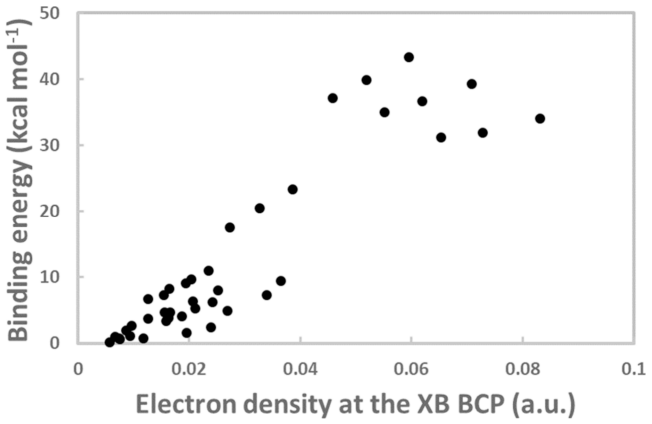

Figure 1. Binding energies versus electron densities at the Bond Critical Points (BCPs) of the halogen bonds (XBs) obtained at the B2PLYP/def2-TZVPD level.

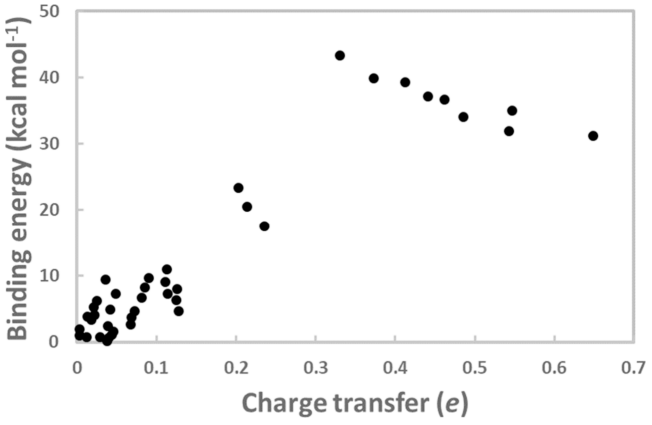

Figure 2. Binding energies vs QTAIM charge transfer values between monomers during halogen bonding obtained at the B2PLYP/def2-TZVPD level.

Previous investigations stablished that the polarizability of the halogen atom directly involved in halogen bonding is positively correlated to the strength of these XBs,[1,2,8] which follows the sequence Cl < Br < I for X as R and B are fixed during the analysis, and our BE values are in agreement with this trend. In other words, the strongest XBs are expected for X = I in each set. Next, again in agreement with the expectations,[1,2,8] it is possible to notice that the electronegativity of the R group in the R−X monomer is quite an important factor to the stabilization of XBs. Hence, the strength of XBs follows the sequence H < I < Br < Cl < F for R, as X and B are kept the same. Previous studies mention that both these factors, larger polarizability of X and increasing electronegativity of R, tend to contribute reinforcing electrostatic and/or covalent stabilization mechanisms of XBs.[6,7] Moreover, the effect of highly electronegative substituents attached to R seems to be transferred along chemical bonds as well once the $-CF_3$ group results in stronger XBs as compared to $-CH_3$, although the direct bonding of X to fluorine still provides higher BEs. Finally, interesting features are observed comparing the Lewis base effect. For example, the sequence of XB strength for anions as bases decreases with ionic radius increments, that is, Cl$^-$ > Br$^-$ > I$^-$. This trend was also noticed before, that is, with weaker XBs for anions with smaller proton affinities, affecting electrostatic and orbital interaction mechanisms of XB stabilization.[7] Moreover, NCH is a more effective base than PCH, although both monomers are inferior to anions, which agrees with discussions in the literature in terms of stronger XBs involving anions as the Lewis base.[2] These findings suggest that smaller and stronger bases (mainly anions) tend to provide a better interaction with the σ-hole. Considering these aspects, it is easy to understand why the highest BE value in this study is that found in the FI···Cl$^-$ dimer. As one could anticipate, exploratory B2PLYP/def2-TZVPD results for FI···F$^-$ predict an even stronger XB, 63.67 kcal mol^{-1}, while DLPNO-CCSD(T)/CBS calculations provide 67.31 kcal mol^{-1}. This is probably the upper limit for such interactions with halogen atoms from fluorine until iodine.

Moreover, as seen in Figure 1, there is an overall trend for achieving stronger XBs as the electron density at the respective BCPs increases, although there are group separations, depending on a common donor or acceptor monomer. This indirect strength descriptor has been successfully used for several chemical bonds and intermolecular interactions, such as

https://doi.org/10.1021/acs.jpca.3c08229
J. Phys. Chem. A XXXX, XXX, XXX−XXX

Table 2. Harmonic Vibrational Frequencies (ω_e) and Fundamental Infrared Intensities (I) for the Stretching Mode of Donor Monomers in Complexes (R−X) and Their Variations on Complexation ($\Delta\omega_e$ and ΔI), as Obtained at the B2PLYP/def2-TZVPD Level and from the CCFDF/QTAIM Model

	B2PLYP/def2-TZVPD				CCFDF/QTAIM	
complex	ω_e (cm^{-1})	$\Delta\omega_e$ (cm^{-1})	I (km mol^{-1})	ΔI (km mol^{-1})	I (km mol^{-1})	ΔI (km mol^{-1})
HCl···Cl$^-$	2917.8	−64.3	54.0	10.2	53.9	10.1
HCl···Br$^-$	2930.3	−51.8	39.7	−4.1	39.7	−4.1
HCl···I$^-$	2940.9	−41.3	29.2	−14.6	29.2	−14.6
HBr···Cl$^-$	2514.2	−152.8	339.6	326.9	339.6	326.8
HBr···Br$^-$	2533.1	−133.8	323.1	310.4	322.9	310.2
HBr···I$^-$	2550.8	−116.1	317.3	304.6	316.9	304.2
HI···Cl$^-$	2098.3	−249.4	743.1	743.1	743.1	743.1
HI···Br$^-$	2117.8	−229.8	795.8	795.8	795.7	795.7
HI···I$^-$	2132.8	−214.8	907.0	907.0	906.2	906.2
FCl···Cl$^-$	410.4	−376.2	439.9	409.8	439.9	409.8
FCl···Br$^-$	395.3	−391.3	510.2	480.1	510.2	480.1
FCl···I$^-$	366.9	−419.8	541.3	511.2	541.2	511.1
FBr···Cl$^-$	407.1	−267.2	277.9	246.5	277.9	246.5
FBr···Br$^-$	395.6	−278.6	353.8	322.4	353.8	322.4
FBr···I$^-$	372.8	−301.4	412.1	380.7	412.0	380.6
FI···Cl$^-$	411.2	−200.8	228.2	184.7	228.2	184.7
FI···Br$^-$	406.0	−206.0	286.3	242.9	286.3	242.9
FI···I$^-$	392.7	−219.3	344.0	300.5	343.9	300.5
Br_2···NCH	316.7	−10.1	4.8	4.8	4.8	4.8
Br_2···PCH	323.0	−3.9	0.9	0.9	0.9	0.9
BrI···NCH	259.2	−12.1	12.3	10.9	12.3	10.7
ClBr···NCH	427.5	−17.4	15.5	14.0	15.5	14.0
ClI···NCH	368.7	−19.9	30.7	23.4	30.7	23.4
FBr···NCH	628.2	−46.0	103.6	72.2	103.6	72.2
FI···NCH	571.1	−40.9	109.7	66.2	109.7	66.2
HBr···NCH	2657.5	−9.4	2.4	−10.4	2.4	−10.4
HI···NCH	2329.2	−18.4	8.3	8.3	8.3	8.3
I_2···NCH	213.0	−6.6	3.7	3.7	3.7	3.7
FCl···NCH	738.0	−48.7	110.0	79.8	109.9	79.8
FI···PCH	583.5	−28.5	113.3	69.8	113.3	69.8
FBr···PCH	643.9	−30.3	97.5	66.1	97.5	66.1
FCl···PCH	764.3	−22.4	80.3	50.2	80.3	50.2
CH_3I···Cl$^-$	490.9	−52.5	58.2	55.3	57.8	55.0
CH_3I···Br$^-$	493.8	−49.6	64.7	61.8	62.9	60.1
CH_3I···I$^-$	494.7	−48.7	73.1	70.2	73.4	70.6
CF_3Cl···Cl$^-$	449.7	−21.4	39.3	39.1	39.2	39.0
CF_3Cl···Br$^-$	452.8	−18.4	34.7	34.5	30.9	30.6
CF_3Cl···I$^-$	454.9	−16.2	30.3	30.1	30.8	30.5
CF_3I···Cl$^-$	234.3	−53.6	41.3	41.3	41.4	41.4
CF_3I···Br$^-$	223.3	−64.7	60.6	60.6	58.8	58.7
CF_3I···I$^-$	229.2	−58.7	73.8	73.7	70.5	70.5

hydrogen bonds as well.[47] Hence, the electron density values at the BCPs can also be used for the fast evaluation of XBs. However, our results presented in Table S2 (see the Supporting Information) suggest that better linear correlations might be obtained for each pair of X···B atoms involved in halogen bonding, recommending the need for constructing different models to attain more reliable strength predictions of XB interactions. Of course, the number of points in these individual regressions is small to draw a more definitive conclusion.

Atomic charges from QTAIM can also be used to evaluate the electronic charge transfer (CT) process that occurs between the monomers during halogen bonding (Table 1). As mentioned before, this quantity has been frequently ascribed to covalent 3c-4e contributions to XBs,[6] although polarization also leads to significant CT in these systems.[48] First, in accordance with the literature,[1] one can notice that the XB donor monomer (Lewis acid) always receives some electronic charge from the XB acceptor (Lewis base), with CT values reaching up to 0.65 e (FCl···I$^-$). For comparison, CT results obtained with QTAIM for HBs in complexes like HF···HF, HCl···HCl, HCN···HCN, HNC···HNC, HCN···HF, HF···HCl, and H_2O···HF, with BEs between 1.45 and 7.79 kcal mol^{-1}, vary between from 0.004 to 0.030 e.[18] If we analyze only our neutral systems, which present comparable BEs, the CT results are between 0.002 and 0.048 e.

By far, the most significant CT amounts are always seen in F−X′···X$^-$ and CF_3I···X$^-$ complexes (X′, X = Cl, Br, and I), that is, those presenting the strongest XBs. As expected, these F−X′···X$^-$ systems tend to exhibit short XBs. Hence, anions

https://doi.org/10.1021/acs.jpca.3c08229
J. Phys. Chem. A XXXX, XXX, XXX−XXX

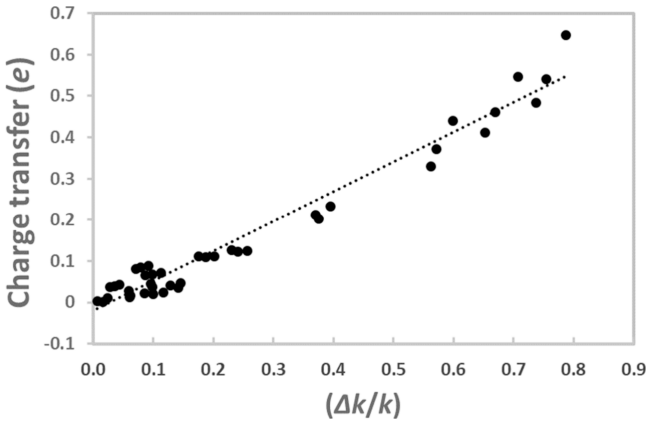

Figure 3. QTAIM charge transfer values between monomers during halogen bonding versus $\Delta k/k$ data (see text) obtained at the B2PLYP/def2-TZVPD level.

are much more efficient bases to enhance CT contributions to BEs and this capability clearly increases with the ionic radius in F−X′···X$^-$ and CF_3I···X$^-$ complexes, that is, Cl$^-$ < Br$^-$ < I$^-$. Overall, although a direct relationship between CT results and BEs is not achieved, one can see in Figure 2 that there is a crude trend for stronger halogen bonding as CT is enhanced. In fact, the pattern seen in this figure for the F−X′···X$^-$ complexes suggests that electrostatic contributions to the XBs are majorly responsible for the dispersion noticed in the points of Figure 2.

Harmonic Vibrational Frequencies and Fundamental Infrared Intensities. In the sequence, we discuss the harmonic vibrational frequencies and fundamental infrared intensities obtained for X···B intermolecular stretching modes, as seen in Table S3 (see the Supporting Information). Our calculations are in excellent accordance with the CCSD(T)/ha5Z theoretical values available for HBr···NCH and HI···NCH[12] and with the CCSD(T)/aug-cc-pVTZ results found for FCl···Cl$^-$.[6] These modes are associated with low frequency vibrations (from 35 to 287 cm^{-1}), a characteristic shared by many intermolecular interactions, although the infrared intensities can be moderate (up to 131 km mol^{-1} in FBr···Cl$^-$). The strongest among such bands is observed in XB systems with anions. The CCFDF/QTAIM model provides a nice description of these intensities, with deviations up to 1.5 km mol^{-1} (CF_3Cl···Br$^-$). Hence, almost negligible errors occur in the integrated QTAIM quantities and in the numerical derivative estimates of the charge flux and atomic dipole flux. As seen in Table S4 (see the Supporting Information), the intensity of these modes is largely determined by the sum of three terms involving charge, charge flux, and the interaction between charge and charge flux (C + CF + C × CF), that is, with negligible participation of contributions including dipole flux (atomic polarizations). Fortunately, this mode can be well represented by the sole motion of B with respect to the remaining complex in HCl···Cl$^-$, HBr···Br$^-$, and HI···I$^-$. Thus, analyzing the electronic charge flux in this subset, it is possible to notice that the negatively charged base, which already donated some electronic charge due to CT in the complex formation, loses more electronic charge as this atom moves toward the R−X monomer and this charge amount flows almost entirely to the R atom. Hence, this intermolecular charge flux along the displacement of a negatively charged B atom is capable of explaining the dominating C + CF + C × CF contributions to the intensity of this mode for such complexes.

Next, the vibrational results for the R−X stretching are collected in Table 2, which also exhibits the variations under complexation. First, CCSD(T)/ha5Z values from the literature[12] point to harmonic frequency values for HBr···NCH and HI···NCH of 2661 and 2302 cm^{-1}, with infrared intensities of 2 and 8 km mol^{-1}, respectively, which are in nice agreement with our data. One can notice that the harmonic frequencies always decrease because of the XB formation (red shift), from 3.9 to 419.8 cm^{-1}, while the infrared intensities tend to increase up to 907.0 km mol^{-1} (HI···I$^-$). Similar features were observed before during halogen bonding[1,9,21,22] and also in the X-H stretchings of donor monomers during dimerization by hydrogen bond formation.[18−20] Only a few of the systems investigated here show slightly weaker R−X bands due to halogen bonding, namely, HCl···Br$^-$, HCl···I$^-$, and HBr···NCH. Once again, the CCFDF/QTAIM model provides a nice description of the infrared intensities for this mode, with deviations up to 3.8 km mol^{-1} or 11% (CF_3Cl···Br$^-$). Apart from this case, the deviations decrease to 3.3 km mol^{-1} or 4.5% (CF_3I···I$^-$).

The red shift denotes that the R−X bonds are becoming less stiff, which may also suggest some bond weakening. In the literature, this has been frequently interpreted by means of the Mulliken's charge transfer model,[49] that is, as the result of some electronic charge donation from the Lewis base to the unoccupied antibonding σ orbital (σ^*) from R−X.[1,3] This provides a B$^+$···[X−R]$^-$ resonance structure.[22] However, an alternative resonance structure has also been cogitated for these systems, [B−X]$^+$···R$^-$, which is explained by considering a more or less strong localization of the antibonding orbital on R.[21] Thus, the increasing participation of both ionic structures in the description of the complex is expected to lead to the red shift observed.[22] Indeed, to further explore this idea, the correlation plots of Huggins and Pimentel can be used.[22,50] Thus, force constants (k) for the R−X stretching mode, presented in Table S5 (see the Supporting Information), are used to calculate $(k_{donor} - k_{complex})/k_{donor} = \Delta k/k$. Figure 3 shows the relation between $\Delta k/k$ and CT (see Table 1). As one can see, the linear correlation is nice, with a coefficient of determination (R^2) of 0.96, which agrees with the ideas previously discussed. Thus, the participation of these ionic structures compared to the B···X−R neutral one is predicted to be predominating for F−X′···X$^-$ complexes (more than 50%), which requires CT amounts larger than 0.3 e.

The values in Table 3 are presented to evaluate the infrared intensity variations observed on the XB formation. Alone, the contribution that exhibits the best correlation with the infrared intensity changes is the interaction term between charge flux and dipole flux (CF × DF), with R^2 = 0.70 in linear regressions. If this contribution is summed with the interaction term between charge and charge flux (C × CF + CF × DF), the R^2 value increases to 0.93, as illustrated in Figure 4. Hence, this feature is quite different from the picture that emerged on hydrogen bonding, where infrared intensity increments on dimerization are usually dominated by the C × CF contribution.[18,20] In fact, the dynamic terms now seem to be much more important for systems with XBs. Moreover, the CCFDF/QTAIM analysis shows that a model lacking atomic dipole fluxes is not able of properly describing this intensity strengthening for the R−X stretching during the XB formation, as done in the past with effective charges.[22] More recently,

https://doi.org/10.1021/acs.jpca.3c08229
J. Phys. Chem. A XXXX, XXX, XXX−XXX

Table 3. Variations of the Fundamental Infrared Intensities (ΔI) for the Stretching Mode of Donor Monomers (R−X) on Complexation, as Obtained from the CCFDF/QTAIM Model Based on B2PLYP/def2-TZVPD Calculations (in km mol^{-1})

	CCFDF/QTAIM								B2PLYP
complex	ΔC	ΔCF	ΔDF	Δ(C × CF)	Δ(C × DF)	Δ(CF × DF)	Δtotal	Δ(C × CF) + Δ(CF × DF)	Δtotal
HCl···Cl$^-$	−40.1	−71.5	6.2	−195.4	53.6	257.3	10.1	61.9	10.2
HCl···Br$^-$	−36.0	−74.6	6.2	−186.3	46.6	239.9	−4.1	53.6	−4.1
HCl···I$^-$	−31.4	−76.0	4.3	−180.0	40.4	228.0	−14.6	48.0	−14.6
HBr···Cl$^-$	−15.6	−371.1	−28.7	−152.3	144.4	750.0	326.8	597.7	326.9
HBr···Br$^-$	−15.2	−371.0	−23.4	−151.9	129.2	742.5	310.2	590.6	310.4
HBr···I$^-$	−14.4	−371.1	−23.8	−152.2	112.2	753.4	304.2	601.2	304.6
HI···Cl$^-$	40.9	−477.0	−11.8	131.0	162.8	897.1	743.1	1028.1	743.1
HI···Br$^-$	35.4	−471.5	−11.4	147.4	147.4	948.4	795.7	1095.8	795.8
HI···I$^-$	29.7	−450.7	−20.4	176.1	127.0	1044.5	906.2	1220.6	907.0
FCl···Cl$^-$	1.1	93.2	−123.4	171.7	−56.9	324.1	409.8	495.8	409.8
FCl···Br$^-$	0.7	171.8	−129.2	189.0	−64.2	312.0	480.1	501.0	480.1
FCl···I$^-$	−1.0	264.0	−135.1	199.1	−77.1	261.2	511.1	460.3	511.2
FBr···Cl$^-$	2.8	14.8	−56.5	121.8	−30.2	193.8	246.5	315.6	246.5
FBr···Br$^-$	4.5	57.8	−60.0	145.7	−32.0	206.3	322.4	352.0	322.4
FBr···I$^-$	4.0	117.9	−67.3	167.2	−41.5	200.3	380.6	367.5	380.7
FI···Cl$^-$	3.5	−1.5	−20.3	91.9	−10.7	121.8	184.7	213.7	184.7
FI···Br$^-$	5.6	18.0	−21.5	111.5	−9.6	138.9	242.9	250.4	242.9
FI···I$^-$	5.4	52.9	−27.8	134.2	−16.2	151.9	300.5	286.1	300.5
Br_2···NCH	0.1	3.7	0.0	1.0	0.0	0.1	4.8	1.1	4.8
Br_2···PCH	0.0	1.0	0.0	0.0	0.0	−0.2	0.9	−0.2	0.9
BrI···NCH	−0.7	8.6	−4.7	2.0	−3.6	9.1	10.7	11.1	10.9
ClBr···NCH	0.7	−4.7	−0.8	4.7	1.3	12.7	14.0	17.4	14.0
ClI···NCH	1.7	−12.8	−3.1	9.8	2.0	25.8	23.4	35.6	23.4
FBr···NCH	2.6	−45.8	−15.3	39.0	−2.2	93.9	72.2	132.9	72.2
FI···NCH	3.7	−23.7	−7.1	35.5	0.4	57.4	66.2	92.9	66.2
HBr···NCH	−5.0	−39.2	11.8	−33.4	25.2	30.3	−10.4	−3.1	−10.4
HI···NCH	4.9	−85.0	0.9	−22.2	32.0	77.8	8.3	55.6	8.3
I_2···NCH	0.1	2.6	0.0	0.8	0.0	0.2	3.7	1.0	3.7
FCl···NCH	1.3	−83.5	−33.5	44.2	−7.4	158.7	79.8	202.9	79.8
FI···PCH	1.4	−24.4	−8.2	40.6	−3.6	64.0	69.8	104.6	69.8
FBr···PCH	0.6	−45.2	−13.9	38.8	−5.4	91.3	66.1	130.1	66.1
FCl···PCH	0.0	−64.9	−17.7	30.4	−5.6	108.0	50.2	138.4	50.2
CH_3I···Cl$^-$	2.4	−108.2	−15.9	4.1	16.6	156.0	55.0	160.1	55.3
CH_3I···Br$^-$	2.3	−109.0	−15.7	5.2	16.5	160.9	60.1	166.1	61.8
CH_3I···I$^-$	1.9	−110.1	−18.3	8.2	14.1	174.8	70.6	183.0	70.2
CF_3Cl···Cl$^-$	6.5	31.1	3.0	50.6	−9.1	−43.1	39.0	7.5	39.1
CF_3Cl···Br$^-$	6.1	26.8	4.9	46.9	−10.9	−43.1	30.6	3.8	34.5
CF_3Cl···I$^-$	5.2	30.8	6.9	48.5	−12.1	−48.9	30.5	−0.4	30.1
CF_3I···Cl$^-$	1.6	−13.9	−2.4	30.2	−1.5	27.5	41.4	57.7	41.3
CF_3I···Br$^-$	3.2	−7.6	−3.1	38.0	−1.7	29.9	58.7	67.9	60.6
CF_3I···I$^-$	2.6	1.9	−4.0	43.8	−4.0	30.3	70.5	74.1	73.7

efforts to understand this band strengthening on halogen bonding have also been done by including charge flux in the interpretation.[23−25] These investigations argued that the intermolecular charge flux from B to the donor monomer is responsible for the observed infrared intensity enhancement observed. However, the atomic dipole flux was not considered again.

Certainly, the R−X stretching mode in a XB system can be much more complicated than the X−H stretching mode of HB complexes. In fact, due to the small atomic mass of hydrogen, the X−H stretching mode is approximately represented by the sole motion of this light atom. However, in XB complexes, the R−X stretching mode frequently involves significant displacements of other atoms as well, as seen in H_3C−I···B, F_3C−Cl···B, and F_3C−I···B complexes. Moreover, in many of the XB complexes investigated here, the R atom tends to take place in much larger displacements than X during this stretching mode because of their masses, which occurs, for instance, in the H−X···B and F−I···B complexes.

Anyway, as seen in Table S5 (see the Supporting Information), while the donor monomers follow a common behavior resulting from the negative correlation normally seen between charge flux and atomic dipole flux contributions to dipole moment derivatives of vibrational modes,[15,17] a pattern noticed as well for the X−H stretching mode of HB complexes,[18] the same does not occur for the R−X stretching mode in many XB systems, mainly for those with anions as Lewis bases. The usual behavior observed in several different systems is characterized by proportional CF and DF contributions along with a negative CF × DF term and inversely correlated C × CF and C × DF contributions, being closely related to the counter polarization idea discussed by

https://doi.org/10.1021/acs.jpca.3c08229
J. Phys. Chem. A XXXX, XXX, XXX−XXX

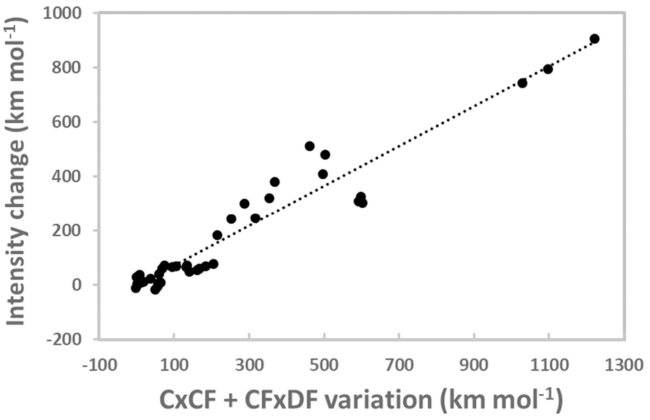

Figure 4. Changes in fundamental infrared intensities due to halogen bonding versus the sum of contributions to these variations due to interaction terms between charge and charge flux (C × CF) plus charge flux and dipole flux (CF × DF) obtained at the B2PLYP/def2-TZVPD level.

Bader and Matta for equilibrium geometries.[51] In other words, the transfer of electronic charge from one point of a molecular system to another one is frequently accompanied by counter polarization effects in the opposite direction, which are described by atomic dipole fluxes. This process is obviously in accordance with a purely electrostatic point of view of electronic charge movements in molecular systems.

On the other hand, CF and DF terms are no longer proportional to each other during R−X stretchings in XB complexes. In general, there is not an inverse correlation between C × CF and C × DF contributions and the CF × DF term can be largely positive (reaching 199.1 km mol^{-1} in HI···I$^-$) for these systems. Anyway, even for the complexes with negative CF × DF values in Table S5 (majorly those with neutral bases), the halogen bonding almost always causes an increment of this contribution (except mainly for CF_3Cl···B systems with anions as bases), as seen in Table 3. This is surprising and suggests the existence of an unusual electronic charge flow mechanism operating in R−X stretchings of XB complexes.

Atomic Interpretation of Electronic Structure Changes in R−X Stretchings. First, one can analyze the atomic charges obtained from QTAIM for the equilibrium geometries, which are displayed in Table 4. Normally, the atom of the Lewis base that interacts directly on halogen bonding is negatively charged, except in PCH. The phosphorus atom in this molecule shows a highly positive QTAIM charge (1.2 e), although it can still act as a Lewis base due to the largely asymmetric electron cloud with a prominent lone pair evidenced in the atomic dipole moment values. The charges of the R group tend to be negative in almost all complexes except for the HCl···X$^-$, HBr···X$^-$, and HBr···NCH systems (carbon can also be positively charged in CF_3Cl···X$^-$ and CF_3I···X$^-$, although fluorine atoms are negatively charged). On the other hand, the X halogen usually shows positive charges in the XB complexes, except for HCl···X$^-$, HBr···X$^-$, FCl···I$^-$, Br_2···PCH, HBr···NCH, and CF_3Cl···X$^-$. Certainly, a positive charge on X can contribute to enhance the electrostatic stabilization of the complex with the Lewis base.[7]

The variations in charge values on halogen bonding are shown in Table 5. As mentioned before, the XB donor (Lewis acid) receives an electronic charge from the XB acceptor (Lewis base), although the atomic contributions deserve a more careful investigation. For example, the electronic charge received by the Lewis acid goes preferentially to the R moiety, reaching even to the other atoms along the $-CH_3$ and $-CF_3$ groups, and the X atom tends to lose some electronic charge on XB formation, except majorly for F−X···B complexes (X = Cl, Br, and I) with anions as bases, which are characterized by donations to the entire R−X monomer (mainly to the X atoms). The donation of electronic charge to both the atoms of these R−X monomers suggests a predominance of the B$^+$··· [X−R]$^-$ ionic resonance structure, while [B−X]$^+$···R$^-$ seems important for the other cases, although both alternatives probably contribute in all systems. In the case of neutral molecular bases, NCH and PCH, the electronic charge donated on halogen bonding is provided by carbon and hydrogen (probably as the result of internal rearrangements in the base), while nitrogen and phosphorus can become more negatively charged in the process.

Next, Tables S6 and S7 (see the Supporting Information) present atomic dipole moment components from QTAIM along the B···X−R axis, with R at the positive end, and their changes on XB formation. According to these results, the electronic charge received by R on halogen bonding tends to be more accumulated at the opposite side of the R−X bond, as indicated by these atomic dipole variations on halogen bonding, which are frequently negative. In addition, the electronic charge donated by B seems to be retrieved from the atomic basin region toward X (positive atomic dipole changes on XB formation). Certainly, this is in accordance with the expectations of electronic charge transfer from the lone pair of B to the unoccupied σ^* orbital of R−X. However, the variations in the atomic dipole of X under halogen bonding are not easy to interpret once the approximation of the Lewis base will contribute to changes in this quantity and the two ionic resonance structures can exhibit comparable participations in these XB systems. In other words, polarization effects such as the ones evidenced in electron density difference (EDD) maps for red shift XB complexes can also be almost as important as 3c-4e covalent contributions to the XBs, being probably capable of populating the σ^* orbital of R−X as well.[48]

Next, as seen in Table S8 (see the Supporting Information), more concise information can be obtained from dipole moment derivative contributions to the R−X stretching mode (Q_{R-X}) along this r chemical bond axis ($\partial\mu_r/\partial Q_{R-X}$), as partitioned according to the CCFDF/QTAIM method. In this case, the mode is represented by a bond enlargement with the R group placed on the positive side of the r axis. One can see that the largest variations during halogen bonding occur in the CF contribution (the charge flux direction can be completely reversed because of the XB formation), with only minor changes occurring in C and DF terms. Almost all complexes present negative DF contributions to $\partial\mu_r/\partial Q_{R-X}$, except for Br_2···PCH, CF_3Cl···Cl$^-$, CF_3Cl···Br$^-$, and CF_3Cl···I$^-$, and the CF contribution variations due to halogen bonding are always negative. Certainly, this pattern agrees nicely with the reinforcing picture of both contributions to the infrared intensities of the R−X stretching on XB formation, providing positive variations of CF × DF terms for almost all complexes on halogen bonding (see Table 3), except for the ones with positive DF values to $\partial\mu_r/\partial Q_{R-X}$.

Fortunately, as discussed before, the R−X stretching modes of H−X···B and F−I···B complexes can be nicely represented by the displacement of a light atom along the r axis, which is

https://doi.org/10.1021/acs.jpca.3c08229
J. Phys. Chem. A XXXX, XXX, XXX−XXX

Table 4. QTAIM Charges Obtained at the B2PLYP/def2-TZVPD Level (in e)

	donor					acceptor		
complex	X	R	H,F	H,F	H,F	B	C	N
HCl···Cl^-	−0.256	0.213				−0.957		
HCl···Br^-	−0.262	0.223				−0.960		
HCl···I^-	−0.270	0.233				−0.962		
HBr···Cl^-	−0.080	0.007				−0.928		
HBr···Br^-	−0.089	0.021				−0.932		
HBr···I^-	−0.102	0.035				−0.933		
HI···Cl^-	0.111	−0.223				−0.888		
HI···Br^-	0.098	−0.209				−0.889		
HI···I^-	0.081	−0.194				−0.887		
FCl···Cl^-	0.118	−0.604				−0.515		
FCl···Br^-	0.055	−0.597				−0.458		
FCl···I^-	−0.046	−0.603				−0.352		
FBr···Cl^-	0.249	−0.660				−0.588		
FBr···Br^-	0.191	−0.652				−0.539		
FBr···I^-	0.103	−0.650				−0.453		
FI···Cl^-	0.405	−0.735				−0.670		
FI···Br^-	0.355	−0.728				−0.628		
FI···I^-	0.282	−0.723				−0.559		
Br_2···NCH	0.043	−0.060				−1.168	0.952	0.233
Br_2···PCH	−0.004	−0.009				1.155	−1.305	0.162
BrI···NCH	0.240	−0.260				−1.186	0.966	0.240
ClBr···NCH	0.178	−0.200				−1.170	0.957	0.235
ClI···NCH	0.363	−0.388				−1.190	0.971	0.243
FBr···NCH	0.485	−0.534				−1.175	0.977	0.246
FI···NCH	0.606	−0.641				−1.202	0.986	0.252
HBr···NCH	−0.107	0.104				−1.158	0.937	0.224
HI···NCH	0.107	−0.109				−1.168	0.943	0.227
I_2···NCH	0.062	−0.074				−1.179	0.957	0.235
FCl···NCH	0.394	−0.436				−1.161	0.964	0.238
FI···PCH	0.571	−0.609				1.152	−1.291	0.178
FBr···PCH	0.454	−0.499				1.169	−1.296	0.173
FCl···PCH	0.378	−0.406				1.164	−1.302	0.166
CH_3I···Cl^-	0.091	−0.239	0.007	0.007	0.007	−0.874		
CH_3I···Br^-	0.073	−0.234	0.012	0.012	0.012	−0.875		
CH_3I···I^-	0.049	−0.230	0.018	0.018	0.018	−0.872		
CF_3Cl···Cl^-	−0.030	1.915	−0.658	−0.658	−0.658	−0.910		
CF_3Cl···Br^-	−0.045	1.931	−0.657	−0.657	−0.657	−0.915		
CF_3Cl···I^-	−0.063	1.949	−0.656	−0.656	−0.656	−0.918		
CF_3I···Cl^-	0.247	1.572	−0.674	−0.674	−0.674	−0.797		
CF_3I···Br^-	0.216	1.588	−0.673	−0.673	−0.673	−0.786		
CF_3I···I^-	0.174	1.605	−0.671	−0.671	−0.671	−0.765		

hydrogen or fluorine, respectively, for both molecular groups. Thus, these systems provide simpler models for understanding $\partial\mu_r/\partial Q_{R-X}$ changes, which can be assessed by the CCFDF/QTAIM analysis of a single APT element of the light atom ($\partial\mu_r/\partial r_R$). Thus, some components of eqs 2 and 3 are shown in Table 6. First, the charge of R is slightly smaller in the complex, which results in only minor C contributions to changes in $\partial\mu_r/\partial Q_{R-X}$ due to halogen bonding. In the sequence, one can see that the Lewis base donates more electronic charge as the R−X bond of the XB complex is stretched, which is transferred mainly to R (X can receive or lose small amounts of electronic charge in this process). This is opposite to the normal situation found in isolated donor monomers, where R always loses some electronic charge to X in the same stretching mode (positive CF contributions to $\partial\mu_r/\partial r_R$), explaining why the CF contribution to $\partial\mu_r/\partial Q_{R-X}$ becomes less positive or negative on halogen bonding. Moreover, as R and B are separated by two bonds (R−X and X···B), this charge flux change results in predominating effects to $\partial\mu_r/\partial Q_{R-X}$ variations on XB formation (see eqs 2−4), providing even reversed charge flux directions for some complexes. This is an intermolecular charge flux phenomenon, evidencing another difference with respect to simple HBs studied before, which exhibit predominant charge flux changes on dimerization occurring inside the donor monomer structure along the X−H stretching mode.[18] The most relevant DF contribution to $\partial\mu_r/\partial r_R$ in these monomers and dimers is by far the one ascribed to X, which is negative. Of course, a more polarizable halogen is important for stronger XBs and it is not surprising that the polarization changes of X predominate along this stretching mode. In addition, the halogen bonding tends to cause insignificant variations in these dipole fluxes, explaining the small changes in DF terms for $\partial\mu_r/\partial Q_{R-X}$ on XB formation. However, since the most important dipole flux

https://doi.org/10.1021/acs.jpca.3c08229
J. Phys. Chem. A XXXX, XXX, XXX−XXX

Table 5. QTAIM Charge Changes during Complexation with XB Formation Obtained at the B2PLYP/def2-TZVPD Level (in *e*)

	donor					acceptor		
complex	X	R	H,F	H,F	H,F	B	C	N
HCl···Cl^-	0.038	−0.081				0.043		
HCl···Br^-	0.031	−0.071				0.040		
HCl···I^-	0.023	−0.061				0.038		
HBr···Cl^-	0.047	−0.119				0.072		
HBr···Br^-	0.037	−0.106				0.068		
HBr···I^-	0.025	−0.091				0.067		
HI···Cl^-	0.029	−0.141				0.112		
HI···Br^-	0.016	−0.127				0.111		
HI···I^-	−0.001	−0.112				0.113		
FCl···Cl^-	−0.283	−0.203				0.485		
FCl···Br^-	−0.346	−0.196				0.542		
FCl···I^-	−0.447	−0.202				0.648		
FBr···Cl^-	−0.237	−0.174				0.412		
FBr···Br^-	−0.295	−0.166				0.461		
FBr···I^-	−0.382	−0.164				0.547		
FI···Cl^-	−0.183	−0.146				0.330		
FI···Br^-	−0.233	−0.139				0.372		
FI···I^-	−0.306	−0.135				0.441		
Br_2···NCH	0.043	−0.060				−0.015	0.021	0.012
Br_2···PCH	−0.004	−0.009				−0.001	0.008	0.006
BrI···NCH	0.057	−0.077				−0.033	0.034	0.019
ClBr···NCH	0.037	−0.060				−0.018	0.026	0.014
ClI···NCH	0.047	−0.071				−0.038	0.040	0.022
FBr···NCH	−0.001	−0.048				−0.022	0.046	0.025
FI···NCH	0.018	−0.053				−0.049	0.054	0.031
HBr···NCH	0.019	−0.022				−0.005	0.006	0.003
HI···NCH	0.024	−0.027				−0.016	0.012	0.006
I_2···NCH	0.062	−0.074				−0.027	0.026	0.014
FCl···NCH	−0.007	−0.035				−0.008	0.032	0.017
FI···PCH	−0.017	−0.021				−0.004	0.021	0.021
FBr···PCH	−0.032	−0.014				0.013	0.017	0.016
FCl···PCH	−0.023	−0.005				0.008	0.011	0.010
CH_3I···Cl^-	0.080	−0.037	−0.056	−0.056	−0.056	0.126		
CH_3I···Br^-	0.062	−0.032	−0.051	−0.051	−0.051	0.125		
CH_3I···I^-	0.038	−0.028	−0.046	−0.046	−0.046	0.128		
CF_3Cl···Cl^-	0.103	−0.153	−0.013	−0.013	−0.013	0.090		
CF_3Cl···Br^-	0.087	−0.137	−0.012	−0.012	−0.012	0.085		
CF_3Cl···I^-	0.069	−0.119	−0.010	−0.010	−0.010	0.082		
CF_3I···Cl^-	0.078	−0.211	−0.023	−0.023	−0.023	0.203		
CF_3I···Br^-	0.047	−0.196	−0.022	−0.022	−0.022	0.214		
CF_3I···I^-	0.005	−0.178	−0.020	−0.020	−0.020	0.235		

contribution to $\partial\mu_r/\partial r_R$ is negative (from polarization changes of X during these vibrations), the electronic charge flux direction changes on complexation previously mentioned (from B to R) now reinforce dipole moment derivative contributions from the atomic dipoles, providing positive CF × DF terms that are mainly responsible for the infrared intensity strengthening of R−X stretchings due to halogen bonding. Hence, this intermolecular charge flux is now aligned with the predominant atomic dipole flux component from X.

However, one important question still remains. Why does the atomic dipole flux along the R−X stretchings remain almost unaltered under halogen bonding? Although the atomic dipoles were not explicitly considered by Torii, this author also found evidence from electron density analyses that intramolecular polarizations (closely associated with atomic dipole fluxes) do not provide relevant cancellations with the charge flux contribution in an analogous stretching mode of another XB complex (C_6F_5I···$NC_5H_4CH_3$).[25] Certainly, as X is usually more susceptible to polarization changes in these stretchings (see Table 6), any atomic dipole flux changes should affect mainly this atom, with concomitant variations to $\partial m_{X,r}/\partial r_R$ values. According to the charge flow−counter polarization idea and considering the charge fluxes mentioned before, this atomic dipole flux was expected to increase on complexation (CF becomes less positive or negative, and thus, DF should change in the opposite direction). However, while $\partial m_{X,r}/\partial r_R$ really tends to become slightly more positive during halogen bonding, the variations detected in Table 6 are too small as one takes into consideration the magnitude of charge flux changes. Of course, the charge flow−counter polarization model has some flaws. For example, it does not account for the σ-hole formation once a substituent like fluorine bonded to a

https://doi.org/10.1021/acs.jpca.3c08229
J. Phys. Chem. A XXXX, XXX, XXX−XXX

Table 6. Charge (q_R, in e), Charge Flux ($\partial q_i/\partial r_R$, in e Å^{-1}), and Atomic Dipole Flux ($\partial m_{i,r}/\partial r_R$, in e) Contributions to Dipole Moment Derivatives along the X−R Axis (r) during a Displacement of R ($\partial \mu_r/\partial r_R$) from the CCFDF/QTAIM Partition and Their Variations on Halogen Bond Formation Obtained at the B2PLYP/def2-TZVPD Level[a]

system	q_R	$\partial q_R/\partial r_R$	$\partial q_X/\partial r_R$	$\partial q_B/\partial r_R$	$\partial q_C/\partial r_R$	$\partial q_H/\partial r_R$	$\partial m_{R,r}/\partial r_R$	$\partial m_{X,r}/\partial r_R$	$\partial m_{B,r}/\partial r_R$	$\partial m_{C,r}/\partial r_R$	$\partial m_{H,r}/\partial r_R$
HCl	0.294	0.218	−0.218				0.084	−0.446			
HBr	0.126	0.434	−0.434				0.065	−0.693			
HI	−0.082	0.436	−0.436				0.108	−0.727			
FI	−0.588	0.336	−0.336				0.014	−0.930			
HCl···Cl$^-$	0.213	0.107	−0.169	0.062			0.064	−0.405	−0.032		
HCl···Br$^-$	0.223	0.121	−0.177	0.056			0.066	−0.411	−0.029		
HCl···I$^-$	0.233	0.134	−0.186	0.052			0.068	−0.414	−0.024		
HBr···Cl$^-$	0.007	0.265	−0.382	0.117			0.042	−0.591	−0.056		
HBr···Br$^-$	0.021	0.280	−0.394	0.113			0.042	−0.598	−0.054		
HBr···I$^-$	0.035	0.295	−0.408	0.112			0.042	−0.601	−0.050		
HI···Cl$^-$	−0.223	0.254	−0.403	0.149			0.071	−0.605	−0.074		
HI···Br$^-$	−0.209	0.264	−0.421	0.157			0.070	−0.605	−0.075		
HI···I$^-$	−0.194	0.272	−0.444	0.172			0.066	−0.598	−0.070		
FI···Cl$^-$	−0.735	0.042	−0.313	0.271			−0.025	−0.593	−0.082		
FI···Br$^-$	−0.728	0.045	−0.366	0.321			−0.030	−0.571	−0.075		
FI···I$^-$	−0.723	0.040	−0.429	0.389			−0.037	−0.527	−0.051		
FI···NCH	−0.641	0.235	−0.307	0.001	0.043	0.029	0.007	−0.851	0.000	0.010	−0.002
FI···PCH	−0.609	0.280	−0.378	0.019	0.050	0.030	0.001	−0.865	0.002	0.026	−0.003
HBr···NCH	0.104	0.420	−0.422	−0.004	0	0.002	0.066	−0.699	−0.005	0.001	0.000
HI···NCH	−0.109	0.413	−0.417	−0.007	0.007	0.004	0.111	−0.725	−0.008	0.002	0.000
variations	q_R	$\partial q_R/\partial r_R$	$\partial q_X/\partial r_R$	$\partial q_B/\partial r_R$	$\partial q_C/\partial r_R$	$\partial q_H/\partial r_R$	$\partial m_{R,r}/\partial r_R$	$\partial m_{X,r}/\partial r_R$	$\partial m_{B,r}/\partial r_R$	$\partial m_{C,r}/\partial r_R$	$\partial m_{H,r}/\partial r_R$
HCl···Cl$^-$	−0.081	−0.111	0.049	0.062			−0.019	0.041	−0.032		
HCl···Br$^-$	−0.071	−0.097	0.041	0.056			−0.018	0.036	−0.029		
HCl···I$^-$	−0.061	−0.084	0.032	0.052			−0.016	0.032	−0.024		
HBr···Cl$^-$	−0.119	−0.168	0.052	0.117			−0.023	0.102	−0.056		
HBr···Br$^-$	−0.106	−0.153	0.040	0.113			−0.023	0.095	−0.054		
HBr···I$^-$	−0.091	−0.138	0.026	0.112			−0.023	0.091	−0.050		
HI···Cl$^-$	−0.141	−0.182	0.033	0.149			−0.037	0.122	−0.074		
HI···Br$^-$	−0.127	−0.172	0.015	0.157			−0.038	0.122	−0.075		
HI···I$^-$	−0.112	−0.164	−0.008	0.172			−0.042	0.129	−0.070		
FI···Cl$^-$	−0.146	−0.295	0.024	0.271			−0.038	0.337	−0.082		
FI···Br$^-$	−0.139	−0.292	−0.029	0.321			−0.044	0.359	−0.075		
FI···I$^-$	−0.135	−0.297	−0.092	0.389			−0.051	0.403	−0.051		
FI···NCH	−0.053	−0.102	0.029	0.001	0.043	0.029	−0.007	0.079	0.000	0.010	−0.002
FI···PCH	−0.021	−0.057	−0.042	0.019	0.050	0.030	−0.013	0.065	0.002	0.026	−0.003
HBr···NCH	−0.022	−0.013	0.011	−0.004	0.003	0.002	0.000	−0.006	−0.005	0.001	0.000
HI···NCH	−0.027	−0.023	0.019	−0.007	0.007	0.004	0.003	0.002	−0.008	0.002	0.000

[a]For a bond enlargement displacement with R at the positive side of the r axis.

more polarizable and less electronegative halogen (F−X) acquires a negative charge and, in principle, should deform the electronic cloud of X away from the bond by means of simple electrostatic arguments based on polarizations. Hence, these polarizations are probably transmitted through space (field effect),[52] but the electrons in chemical bonds appear to be the ones really affected by this field. In other words, the polarization in molecular systems seems to be more complicated than expected, and quantum effects may be associated with this unusual behavior.

Hence, the answer for that previous question is probably related to a more efficient charge donation from the Lewis base to the unoccupied σ^* orbital of R−X as this bond is enlarged by small amplitude displacements, as already discussed before in the literature.[7,48] In other words, considering simple arguments driven from atomic orbital combinations used to generate molecular orbitals, one could anticipate that the bonding−antibonding orbital energy separation should decrease as the chemical bond is enlarged (atomic orbital overlap decreases). Hence, as the bonding orbital should be destabilized, the antibonding orbital should be stabilized, making it a more effective electronic charge acceptor. A complicating factor in this analysis is related to the finding that polarization effects can also contribute to charge transfers to the σ^* orbital of R−X, although the role of polarization seems to be a secondary one.[48] In this aspect, the charge flux changes along R−X stretching modes noticed on halogen bonding (increasing electronic charge donation from B to R) are in accordance with the proposal discussed here. Moreover, the variations in the dipole flux of R ($\partial m_{R,r}/\partial r_R$) due to complexation are almost always slightly negative, suggesting that this electronic charge is once again being accumulated preferentially away from the region occupied by the R−X bond, in agreement with the hypothesis. Hence, considering that there is a more effective donation of electronic charge from the Lewis base to the σ^* orbital located mainly on R during the R−X bond enlargement on complexation with XB formation, with an increasing participation of the $[B{-}X]^+\cdots R^-$

https://doi.org/10.1021/acs.jpca.3c08229
J. Phys. Chem. A XXXX, XXX, XXX−XXX

ionic resonance structure, the outcome of small variations in $\partial m_{X,r}/\partial r_R$ values on halogen bonding becomes plausible once there are no relevant electronic charge fluxes to or from X in this process. In other words, a donation of electronic charge from B to the unoccupied σ^* of R−X may not disturb the dipole flux of X if, for instance, the basin characteristics of this halogen atom are not affected substantially by the donation along the stretching. This seems quite reasonable, according to our investigation.

CONCLUSIONS

This study is concerned with the investigation of several simple complexes with XBs (R−X···B; R = substituent group, X = halogen, and B = Lewis base) and properties such as equilibrium geometries, binding energies, vibrational frequencies, and fundamental infrared intensities. Thus, the B2PLYP/def2-TZVPD theoretical approach was successfully employed here, providing results in good agreement with accurate values found in the literature for some of these systems and with benchmark DLPNO-CCSD(T)/CBS binding energy data calculated here. Next, the electron densities and their changes on vibrations are also considered by means of the QTAIM and CCFDF/QTAIM models.

The binding energies are shown to exhibit some correlation with the electron densities at the BCP of such halogen bonds, although there are clear group separations depending on the donor and acceptor monomers. Thus, our results suggest that better models to indirectly access the XB strength based on such electron densities at XB BCPs should be individually constructed for each B···X pair of atoms. Moreover, as expected, the electronic charge transfer from XB acceptors to XB donors given by QTAIM also points to an increment trend of the XB force as CT becomes more important. However, electrostatic contributions to BE values should also be considered for a better description of the XB strength. The increment in CT also seems to be nicely correlated with the decrease in R−X bond stiffness, in agreement with the hypothesis of electronic charge donation from the lone pair of the Lewis base to the unoccupied antibonding σ orbital along R−X.

Despite many similarities observed between XBs and hydrogen bonds, the interpretation for the infrared intensification of the R−X stretching on complexation by XB formation is different from the mechanism discussed for a similar band strengthening also seen for X−H stretchings of the HB donors. Hence, while the charge−charge flux term is usually the most important one for HBs,[18,20] the charge flux−dipole flux contribution predominates for XB systems. Thus, the atomic dipole moment fluxes are crucial to really understand this infrared intensification, and models neglecting this contribution will lead to incomplete or misleading conclusions. This is curious and suggests that the traditional idea of counter polarizations cannot explain this outcome. In fact, upon investigation of a subset of these systems where the R−X stretching can be approximated by the sole displacement of R, there is a more prominent electronic charge flux from B to R during the R−X bond enlargement due to halogen bonding, an intermolecular charge flux, with only small variations in X charges. The atomic dipole fluxes remain nearly unaltered on complexation, being primarily represented by a negative dipole flux of X. Thus, the large charge flux variations due to XB formation in a opposite direction to that seen in isolated donor monomers now reinforce predominant dipole moment fluxes from X, explaining the band strengthening.

Finally, investigating this infrared intensification phenomenon in more detail, it seems that the R−X bond enlargement is increasing the electronic charge donation from the base to the σ^* orbital of the donor monomer, and this is behind the aforementioned charge flux direction change in the complexes, from B to R. The electronic charge received by R seems to be accommodated mainly away from the R−X bond, and as a result, the predominant atomic dipole fluxes of X are only slightly disturbed in the process because this atom is not receiving or donating significant amounts of electronic charge. Hence, the peculiar nature of this intermolecular charge flux phenomenon appears to be responsible for the unusual characteristics observed for the R−X stretching mode on halogen bonding.

ASSOCIATED CONTENT

Supporting Information

The Supporting Information is available free of charge at https://pubs.acs.org/doi/10.1021/acs.jpca.3c08229.

The Supporting Information material contains eight tables presenting equilibrium geometries, additional statistical parameters, vibrational data for the B..X and R−X stretching modes, atomic dipoles from QTAIM, and their variations under halogen bonding (PDF)

AUTHOR INFORMATION

Corresponding Author

Roberto Luiz Andrade Haiduke − *Departamento de Química e Física Molecular, Instituto de Química de São Carlos, Universidade de São Paulo, São Carlos, SP 13560-970, Brazil;* orcid.org/0000-0002-8673-7761; Email: haiduke@iqsc.usp.br

Author

Paulo Eduardo Cavalcanti Martins Filho − *Departamento de Química e Física Molecular, Instituto de Química de São Carlos, Universidade de São Paulo, São Carlos, SP 13560-970, Brazil;* orcid.org/0009-0001-7397-2180

Complete contact information is available at: https://pubs.acs.org/10.1021/acs.jpca.3c08229

Notes

The authors declare no competing financial interest.

ACKNOWLEDGMENTS

The authors thank São Paulo Research Foundation (FAPESP) for financial support (grant 2022/05138-0). R.L.A.H. also is grateful to Brazilian National Council for Scientific and Technological Development (CNPq) for a research grant (306763/2021-4). This study was financed in part by the Coordenação de Aperfeiçoamento de Pessoal de Nível Superior—Brasil (CAPES)—Finance Code 001.

REFERENCES

(1) Cavallo, G.; Metrangolo, P.; Milani, R.; Pilati, T.; Priimagi, A.; Resnati, G.; Terraneo, G. The Halogen Bond. *Chem. Rev.* **2016**, *116*, 2478−2601.

(2) Metrangolo, P.; Meyer, F.; Pilati, T.; Resnati, G.; Terraneo, G. Halogen Bonding in Supramolecular Chemistry. *Angew. Chem., Int. Ed.* **2008**, *47*, 6114−6127.

(3) Costa, P. J. The halogen bond: Nature and applications. *Phys. Sci. Rev.* **2017**, *2*, No. 20170136.
(4) Clark, T.; Hennemann, M.; Murray, J. S.; Politzer, P. Halogen Bonding: The σ-Hole. *J. Mol. Model.* **2007**, *13*, 291−296.
(5) Huber, S. M.; Jimenez-Izal, E.; Ugalde, J. M.; Infante, I. Unexpected trends in halogen-bond based noncovalent adducts. *Chem. Commun.* **2012**, *48*, 7708−7710.
(6) Oliveira, V.; Kraka, E.; Cremer, D. The intrinsic strength of the halogen bond: electrostatic and covalent contributions described by coupled cluster theory. *Phys. Chem. Chem. Phys.* **2016**, *18*, 33031−33046.
(7) Wolters, L. P.; Bickelhaupt, F. M. Halogen Bonding versus Hydrogen Bonding: A Molecular Orbital Perspective. *ChemistryOpen* **2012**, *1*, 96−105.
(8) Politzer, P.; Murray, J. S. σ-Holes vs. Buildups of Electronic Density on the Extensions of Bonds to Halogen Atoms. *Inorganics* **2019**, *7*, 71.
(9) Karpfen, A. Theoretical Characterization of the Trends in Halogen Bonding. *Struct. Bonding (Berlin)* **2008**, *126*, 1−15.
(10) Kozuch, S.; Martin, J. M. L. Halogen Bonds: Benchmarks and Theoretical Analysis. *J. Chem. Theory Comput.* **2013**, *9*, 1918−1931.
(11) Anderson, L. N.; Aquino, F. W.; Raeber, A. E.; Chen, X.; Wong, B. M. Halogen Bonding Interactions: Revised Benchmarks and a New Assessment of Exchange vs Dispersion. *J. Chem. Theory Comput.* **2018**, *14*, 180−190.
(12) Perkins, M. A.; Tschumper, G. S. Characterization of Competing Halogen- and Hydrogen-Bonding Motifs in Simple Mixed Dimers of HCN and HX (X = F, Cl, Br, and I). *J. Phys. Chem. A* **2022**, *126*, 3688−3695.
(13) Bader, R. F. W. *Atoms in Molecules: A Quantum Theory*; Clarendon Press: Oxford, UK, 1990.
(14) Bader, R. F. W. Atoms in Molecules. *Acc. Chem. Res.* **1985**, *18*, 9−15.
(15) Haiduke, R. L. A.; Bruns, R. E. An Atomic Charge−Charge Flux−Dipole Flux Atom-in-Molecule Decomposition for Molecular Dipole-Moment Derivatives and Infrared Fundamental Intensities. *J. Phys. Chem. A* **2005**, *109*, 2680−2688.
(16) Haiduke, R. L. A.; de Paiva Martins Filho, H.; da Silva, A. B. F. A theoretical study on the XeF_2 molecule. *Chem. Phys.* **2008**, *348*, 89−96.
(17) Silva, A. F.; Richter, W. E.; Meneses, H. G. C.; Faria, S. H. D. M.; Bruns, R. E. How Accessible Is Atomic Charge Information from Infrared Intensities? A QTAIM/CCFDF Interpretation. *J. Phys. Chem. A* **2012**, *116*, 8238−8249.
(18) Terrabuio, L. A.; Richter, W. E.; Silva, A. F.; Bruns, R. E.; Haiduke, R. L. A. An atom in molecules study of infrared intensity enhancements in fundamental donor stretching bands in hydrogen bond formation. *Phys. Chem. Chem. Phys.* **2014**, *16*, 24920−24928.
(19) Silva, A. F.; Richter, W. E.; Terrabuio, L. A.; Haiduke, R. L. A.; Bruns, R. E. Quantum theory of atoms in molecules/charge-charge flux-dipole flux models for fundamental vibrational intensity changes on H-bond formation of water and hydrogen fluoride. *J. Chem. Phys.* **2014**, *140*, No. 084306.
(20) da Silva, N. A.; Haiduke, R. L. A. Infrared Intensity Analysis of Hydroxyl Stretching Modes in Carboxylic Acid Dimers by Means of The Charge−Charge Flux−Dipole Flux Model. *J. Comput. Chem.* **2019**, *40*, 2482−2490.
(21) Person, W. B.; Humphrey, R. E.; Deskin, W. A.; Popov, A. I. Infrared Spectra of Iodine Monochloride Charge-transfer Complexes. *J. Am. Chem. Soc.* **1958**, *80*, 2049−2053.
(22) Person, W. B.; Humphrey, R. E.; Popov, A. I. Infrared Spectra of Charge Transfer Complexes. II. Iodine Cyanide Complexes. *J. Am. Chem. Soc.* **1959**, *81*, 273−277.
(23) Torii, H. Intermolecular charge flux as the origin of infrared intensity enhancement upon halogen-bond formation of the peptide group. *J. Chem. Phys.* **2010**, *133*, No. 034504.
(24) Torii, H. Delocalized electrons in infrared intensities. *J. Mol. Struct.* **2014**, *1056−1057*, 84−96.
(25) Torii, H. Correlation of the partial charge-transfer and covalent nature of halogen bonding with the THz and IR spectral changes. *Phys. Chem. Chem. Phys.* **2019**, *21*, 17118−17125.
(26) Frisch, M. J.; Trucks, G. W.; Schlegel, H. B.; Scuseria, G. E.; Robb, M. A.; Cheeseman, J. R.; Scalmani, G.; Barone, V.; Petersson, G. A.; Nakatsuji, H.; et al. *Gaussian 09, Revision D.01*; Gaussian, Inc.: Wallingford CT, 2016.
(27) Grimme, S. Semiempirical hybrid density functional with perturbative second-order correlation. *J. Chem. Phys.* **2006**, *124*, No. 034108.
(28) Weigend, F.; Ahlrichs, R. Balanced basis sets of split valence, triple zeta valence and quadruple zeta valence quality for H to Rn: Design and assessment of accuracy. *Phys. Chem. Chem. Phys.* **2005**, *7*, 3297−3305.
(29) Rappoport, D.; Furche, F. Property-optimized Gaussian basis sets for molecular response calculations. *J. Chem. Phys.* **2010**, *133*, No. 134105.
(30) Peterson, K. A.; Figgen, D.; Goll, E.; Stoll, H.; Dolg, M. Systematically convergent basis sets with relativistic pseudopotentials. II. Small-core pseudopotentials and correlation consistent basis sets for the post-d group 16−18 elements. *J. Chem. Phys.* **2003**, *119*, 11113−11123.
(31) Pritchard, B. P.; Altarawy, D.; Didier, B.; Gibson, T. D.; Windus, T. L. New Basis Set Exchange: An Open, Up-to-Date Resource for the Molecular Sciences Community. *J. Chem. Inf. Model.* **2019**, *59*, 4814−4820.
(32) Diercksen, G. H. F.; Roos, B. O.; Sadlej, A. J. Legitimate calculation of first-order molecular properties in the case of limited CI functions. Dipole moments. *Chem. Phys.* **1981**, *59*, 29−39.
(33) Diercksen, G. H. F.; Sadlej, A. J. Perturbation theory of the electron correlation effects for atomic and molecular properties. Second- and third-order correlation corrections to molecular dipole moments and polarizabilities. *J. Chem. Phys.* **1981**, *75*, 1253−1266.
(34) Handy, N. C.; Schaefer, H. F., III On the evaluation of analytic energy derivatives for correlated wave functions. *J. Chem. Phys.* **1984**, *81*, 5031−5033.
(35) Wiberg, K. B.; Hadad, C. M.; LePage, T. J.; Breneman, C. M.; Frisch, M. J. Analysis of the effect of electron correlation on charge density distributions. *J. Phys. Chem.* **1992**, *96*, 671−679.
(36) Keith, A. *AIMAll (Version 19.10.12), TK Gristmill Software, Overland Park.KS 2016*. Available at: aim.tkgristmill.com (accessed March 10, 2016).
(37) Riplinger, C.; Sandhoefer, B.; Hansen, A.; Neese, F. Natural triple excitations in local coupled cluster calculations with pair natural orbitals. *J. Chem. Phys.* **2013**, *139*, No. 134101.
(38) Riplinger, C.; Neese, F. An efficient and near linear scaling pair natural orbital based local coupled cluster method. *J. Chem. Phys.* **2013**, *138*, No. 034106.
(39) Neese, F. The ORCA program system. *WIREs Comput. Mol. Sci.* **2012**, *2*, 73−78.
(40) Neese, F. Software update: The ORCA program system—Version 5.0. *WIREs Comput. Mol. Sci.* **2022**, *12*, No. e1606.
(41) Weigend, F. Accurate Coulomb-fitting basis sets for H to Rn. *Phys. Chem. Chem. Phys.* **2006**, *8*, 1057−1065.
(42) Weigend, F. Hartree−Fock exchange fitting basis sets for H to Rn. *J. Comput. Chem.* **2008**, *29*, 167−175.
(43) Hellweg, A.; Hättig, C.; Höfener, S.; Klopper, W. Optimized accurate auxiliary basis sets for RI-MP2 and RI-CC2 calculations for the atoms Rb to Rn. *Theor. Chem. Acc.* **2007**, *117*, 587−597.
(44) Zhong, S.; Barnes, E. C.; Petersson, G. A. Uniformly convergent n-tuple-ζ augmented polarized (nZaP) basis sets for complete basis set extrapolations. I. Self-consistent field energies. *J. Chem. Phys.* **2008**, *129*, No. 184116.
(45) Helgaker, T.; Klopper, W.; Koch, H.; Noga, J. Basis-set convergence of correlated calculations on water. *J. Chem. Phys.* **1997**, *106*, 9639−9646.
(46) Neese, F.; Valeev, E. F. Revisiting the Atomic Natural Orbital Approach for Basis Sets: Robust Systematic Basis Sets for Explicitly

https://doi.org/10.1021/acs.jpca.3c08229
J. Phys. Chem. A XXXX, XXX, XXX−XXX

892 Correlated and Conventional Correlated ab initio Methods? *J. Chem.*
893 *Theory Comput.* **2011**, *7*, 33−43.
894 (47) Emamian, S.; Lu, T.; Kruse, H.; Emamian, H. Exploring Nature
895 and Predicting Strength of Hydrogen Bonds: A Correlation Analysis
896 Between Atoms-in-Molecules Descriptors, Binding Energies, and
897 Energy Components of Symmetry-Adapted Perturbation Theory. *J.*
898 *Comput. Chem.* **2019**, *40*, 2868−2881.
899 (48) Wang, C.; Danovich, D.; Shaik, S.; Mo, Y. A Unified Theory for
900 the Blue- and Red-Shifting Phenomena inHydrogen and Halogen
901 Bonds. *J. Chem. Theory Comput.* **2017**, *13*, 1626−1637.
902 (49) Mulliken, R. S. Molecular Compounds and Their Spectra. II. *J.*
903 *Am. Chem. Soc.* **1952**, *74*, 811−824.
904 (50) Huggins, C. M.; Pimentel, G. C. Systematics of the Infrared
905 Spectral Properties of Hydrogen Bonding Systems: Frequency Shift,
906 Half Width and Intensity. *J. Phys. Chem.* **1956**, *60*, 1615−1619.
907 (51) Bader, R. F. W.; Matta, C. F. Atomic Charges Are Measurable
908 Quantum Expectation Values: A Rebuttal of Criticisms of QTAIM
909 Charges. *J. Phys. Chem. A* **2004**, *108*, 8385−8394.
910 (52) K. Macedo, G.; Haiduke, R. L. A. A Quantum Theory Atoms in
911 Molecules Study about the Inductive Effect of Substituents in
912 Methane Derivatives. *ACS Omega* **2020**, *5*, 9041−9045.

https://doi.org/10.1021/acs.jpca.3c08229
J. Phys. Chem. A XXXX, XXX, XXX−XXX